A Modified Model for the Lobula Giant Movement Detector and Its FPGA Implementation

Hongying Meng [a] Kofi Appiah [a] Shigang Yue [a] Andrew Hunter [a]
Mervyn Hobden [b] Nigel Priestley [b] Peter Hobden [b] Cy Pettit [b]

[a] *Department of Computing and Informatics, University of Lincoln, UK*
[b] *E2V Technologies PLC, Lincoln, UK.*

Abstract

The Lobula Giant Movement Detector (LGMD) is a wide-field visual neuron that is located in the Lobula layer of the Locust nervous system. The LGMD increases its firing rate in response to both the velocity of an approaching object and the proximity of this object. It has been found that it can respond to looming stimuli very quickly and can trigger avoidance reactions whenever a rapidly approaching object is detected. It has been successfully applied in visual collision avoidance systems for vehicles and robots. This paper introduces a modified neural model for LGMD that provides additional depth direction information for the movement. The proposed model retains the simplicity of the previous neural network model by adding only a few new cells. It has been simplified and implemented on a reconfigurable computing architecture, Field Programmable Gate Array (FPGA) that takes advantage of the inherent parallelism exhibited by the LGMD. The proposed architecture is designed for general purposes and can work on any FPGA device. The whole system has been tested based on the real-time video streams on a FPGA development board. Experimental results showed that it could respond very quickly with desired outputs working as a fast motion detector.

Key words: Neural networks, Bio-inspired vision chip, Embedded vision, Visual motion, FPGA

1 Introduction

For animals, such as insects, the ability to detect approaching objects is important, serving both to prevent collision as the animal moves and also to avoid capture by predators [15,17]. Evolved over millions of years, the visual collision

avoidance systems in insects are both efficient and reliable. The neural circuits processing visual information in insects are relatively simple compared to those in the human brain and provide an appropriate model for the optical collision avoidance sensors that are needed to equip mobile intelligent machines [11].

The Lobula Giant Movement Detector (LGMD) is a wide-field visual neuron that is located in the Lobula layer of the Locust nervous system. The LGMD increases its firing rate in response to both the velocity of the approaching object and its proximity. It has been found that it can respond to looming stimuli very quickly and can trigger avoidance reactions whenever a rapidly approaching object is detected. It is tightly tuned to respond to objects approaching the locust on a direct collision course [7], but produces little or no response to receding objects [12]. This makes the LGMD an ideal model to develop specialized sensors for automatic collision avoidance[6,1].

A functional neural network based on the LGMD's input circuitry was developed by Rind and Bramwell [16]. This neural network showed the same selectivity as the LGMD neuron for approaching rather than receding objects and responded best to objects approaching on collision rather than near-miss trajectories. The expanding edges of colliding objects and the use of lateral inhibition were the key features of the model. This neural network has also been used to mediate collision avoidance in a real-world environment by incorporating it into the control structure of a miniature mobile robot [3,2].

Inspired by the fact that there are direction selective neurons in the locust [13,14], A new specialized translation-sensitive neural network (TSNN) has been proposed in [21,22]. The proposed TSNN neuron has some common layers with the LGMD model, allowing efficiency savings in the neural computation. The TSNN fuses extracted visual motion cues from several whole field direction selective neural networks, and is only sensitive to translational movements.

TSNN can detect the direction of translation movements very well, but it is not sensitive to movement in depth; LGMD [16,20] detects the direction of movement in depth by both lateral inhibition and feed forward inhibition, where feed forward inhibition plays a critical role in inhibiting LGMD spikes to receding objects. For feed forward inhibition, tune to this role makes it too sensitive to background movements and decreases the sensitivity of LGMD. In this paper, we proposed a modified LGMD model with several extra cells to capture the directional information for depth movements quickly, while the feed forward inhibition cell is only responsible for whole field image movements. We also implement the modified LGMD model on an FPGA platform, confirming its efficiency and ability.

The rest of this paper is organized as follows: In section 2, we give an overview of related work. In section 3, we address the modified LGMD model and its

software simulation. In section 4, we discuss the FPGA design of the proposed model and some experimental results in hardware implementation are given and, finally, we present conclusions.

2 Related work

Visual sensors are becoming increasingly cheap and reliable. This makes it possible for many mobile machines (e.g., mobile robots, cars, boats, planes and some toys) equipped with visual sensors and visual-based navigation systems to avoid unwanted collision automatically in the real world. There have been a number of attempts to design a biospired neural chip based on the LGMD neural network for motion detection.

Laviana et al [8] proposed a vision chip architecture based on the LGMD based neural network model described in [5], that is a simplified model based on the previous LGMD based model proposed in [16,15]. The system includes a block of 100×150 retinotopic units, a controller, a 16Kbits SRAM memory block, I/O registers and some other peripherals needed for addressing, timing control, digital-to analog converters and temperature monitoring. The LGMD based neural model is designed in an FPGA platform and it can deal with 100×150 6-bit input sequences. The chip has been designed in a 0.35μm 2P-2M technology.

Based on the original LGMD based neural model in [16], Okuno and Yagi [9,10] implemented the LGMD neuron on a FPGA platform. It has been designed and implemented as a real-time vision sensor for collision avoidance. The system consist of an analog VLSI silicon retina and the digital FPGA circuit. The system was confirmed to response selectively to colliding objects even in complicated real-world situation.

Both these two implementations for LGMD based neural model were on FPGA, since this is a very good platform for initial chip design. However, there are some limitations in both of them. First, both implementations are based on the original LGMD based neural model, which lacks direction information on the movements. Second, both implementations were highly restricted by their system requirements, since the LGMD model was integrated in the whole system.

In order to explore the high ability and potential of the LGMD neuron, we extend the LGMD based neural model to a modified neural network model that adds depth direction information of the movement. The modified model retains simplicity in the software and hardware implementation. We provide a general FPGA design that can be transferred to any FPGA development

platform. We also integrate the direction information of the movements in depth that makes the design a general motion detector.

3 A modified neural network model for LGMD

The LGMD based neural network proposed in this paper is based on previous studies described in [16,2,18,19]. The modified neural network is shown in figure 1.The LGMD neural network in [16,4,2] was composed of four groups of cells - photoreceptor cells (P); excitatory and inhibitory cells (E and I); summing cells (S), and two single cells - feed-forward inhibition (FFI) and LGMD. The neural network model of LGMD in [19,20] has an extra set of grouping cells between the summing cells and LGMD. This allows clusters of excitation in the summary cells to feed into the LGMD cell, which is useful for collision detection in complex backgrounds.

3.1 Neural network model

The input of the P cells is the luminance change. Lateral inhibition is indicated with dotted lines and has a one frame delay. Excitation is indicated with black lines and has no delay. The FFI also has a one frame delay. The input to FFI is the luminance change from photoreceptor cells. The problem of parameter selection in this LGMD model has been tackled in [23].

The model in [19] works very well for collision detection in complex environments. However, it cannot distinguish the direction of moving objects in depth. For example, the model will respond to both an approaching object and a receding object with high excitation level, especially when an object is very close. In order to enhance the ability to recognize the direction of the moving object in depth, we add a new neural layer with two grouping cells J and H as shown in figure 1. A new cell D is added to give the direction information of the moving object in depth. The proposed neural network (shown in figure 1) used in the paper will be described in detail in the next part (note that the J, H and D cells may not have exact counterparts in real locusts).

3.1.1 P layer

The first layer of the neural network is the photoreceptor P cells arranged in a matrix; the luminance L_f of each pixel in the input image is captured by each photoreceptor cell, the change of luminance P_f between frames of the sequence is calculated and forms the output of this layer. The output of a cell

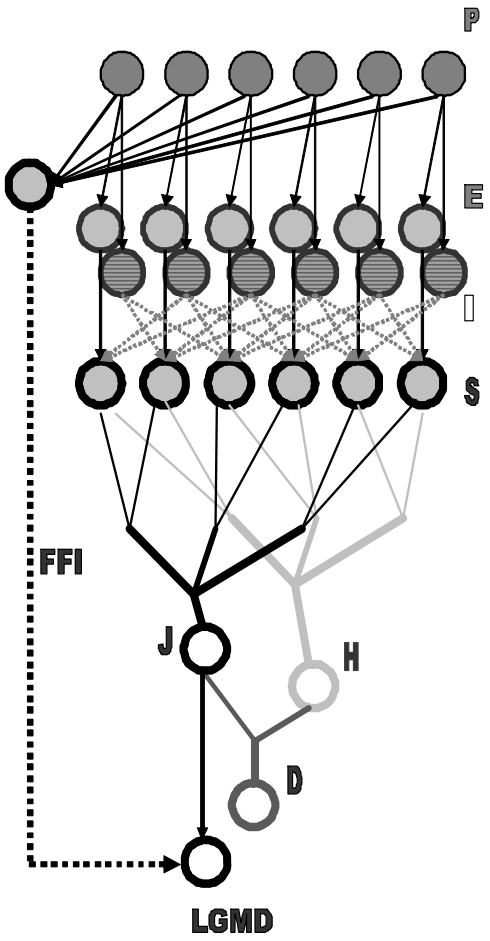

Fig. 1. A schematic illustration of the modified LGMD neural network model. There are four groups of cells and five single cells: photoreceptor cells (P); excitatory and inhibitory cells (E and I); summing cells (S); grouping cells (J and H); depth movement direction cell (D); the LGMD cell and the feed forward inhibition cell (FFI).

in this layer is defined by equation:

$$P_f(x,y) = \sum_{i}^{n_p} p_i P_{f-i}(x,y) + (L_f(x,y) - L_{f-1}(x,y)) \tag{1}$$

where $P_f(x,y)$ is the change of luminance corresponding to pixel (x,y) at frame f, x and y are the index of the matrix, L_f and L_{f-1} are the luminance, subscript f denotes the current frame and $f-1$ denotes the previous frame, n_p defines the maximum number of frames (or time steps) the persistence of the luminance change can last, the persistence coefficient $p_i \in (0,1)$ and

$$p_i(x,y) = (1+e^{\mu i})^{-1} \tag{2}$$

where $\mu \in (-\infty, +\infty)$ and i indicates the previous i^{th} frame counted from the current frame f. Note that the LGMD neural network detects potential collision by responding to expansion of the image edges, a strategy that needs computation rather than a strategy relying on object appearance. If there is no difference between successive images, the P cells are not excited.

3.1.2 I E layer

The output of the P cells forms the inputs to two separate cell types in the next layer. One type are the excitatory cells, through which excitation is passed directly to their retinotopic counterparts in the third layer, the S layer. The excitation $E(x, y)$ in an E cell has the same value as that in the corresponding P cell. The second cell type are lateral inhibition cells, which pass inhibition, after 1 image frame delay, to their retinotopic counterpart's neighboring cells in the S layer with one frame delay. The gathered strength of inhibition of a cell in this layer is given by:

$$I_f(x, y) = \sum_i \sum_j P_{f-1}(x + i, y + j) w_I(i, j), \ (if \ i = j, j \neq 0) \tag{3}$$

where $I_f(x, y)$ is the inhibition corresponds to pixel (x, y) at current frame f, $w_I(i, j)$ is the local inhibition weight. Note that i and j are not allowed to be equal to zero simultaneously. This means inhibition will only be allowed to spread out to its neighboring cells in next layer rather than to its direct counterpart in the next layer.

In our experiments on both software simulation and hardware implementation, the local inhibition weight $w_I(i, j)$ are set to be 0.25 for the four nearest neighbors and 0.125 for the four diagonal neighbors. These values are especially convenient for hardware implementation.

$$w_I = \begin{bmatrix} 0.125 & 0.25 & 0.125 \\ 0.25 & & 0.25 \\ 0.125 & 0.25 & 0.125 \end{bmatrix} \tag{4}$$

3.1.3 S layer

The excitatory flow from the E cells and inhibition from the I cells is summed by the S cells using the following equation:

$$S_f(x, y) = E_f(x, y) - I_f(x, y) W_I \tag{5}$$

where W_I is the inhibition weight. It normally has a value less than 0.8 (0.35 was chosen in all the following experiments).Excitations that exceed a threshold value are able to reach the summation cell LGMD:

$$\tilde{S}_f(x,y) = \begin{cases} S_f(x,y), \, if \;\; S_f(x,y) \geq T_r \\ 0, \qquad\quad if \;\; S_f(x,y) < T_r \end{cases} \tag{6}$$

where T_r is the threshold.

3.1.4 J H cells

The J and H cells are the two new grouping cells for depth movement direction recognition. The J cell is exactly the same as the LGMD cell in the previous LGMD model in terms of spatiotemporal structure and the value it holds. The H cell shares the same structure as the LGMD and J cell, but with a temporal difference. H has one frame delay from J.

$$J_f = \sum_{x,y} \tilde{S}_f(x,y) \tag{7}$$

$$H_f = J_{f-1} \tag{8}$$

3.1.5 D cell

The D cell is used to calculate the difference between the difference of frame f, $f-1$ and $f-2$. It can be represented in the equation 9.

$$D_f = abs(J_f) - abs(H_f) \tag{9}$$

It transpires that D can estimate the depth direction of the moving object very well. When an object is moving away, $abs(J_f)$ is always smaller than $abs(H_f)$. When an object is approaching, $abs(J_f)$ is bigger than $abs(H_f)$. In order to distinguish slow movements we add a threshold T_D for D_f. We then get a simple variable $\tilde{D}$ that has only three values: '0', '1' and '-1', where '1' stands for approaching, '-1' stands for receding and '0' stands for no significant movements. The threshold T_D mainly depends on the size of the image frame. It will be set bigger if the image size is bigger.

$$\tilde{D}_f = \begin{cases} 1, \quad if \;\; D_f \geq T_D \\ 0, \quad if \;\; -T_D < D_f < T_D \\ -1, \, if \;\; D_f \leq -T_D \end{cases} \tag{10}$$

With the above cells, the LGMD model can recognize directional information for depth movements quickly. The feed forward inhibition cell, as detailed later, is able to concentrate on whole image movements to avoid perturbation from background movements.

3.1.6 LGMD cell

The membrane potential J is then transformed to a spiking output using a sigmoid transformation,

$$LGMD_f = (1 + e^{-J_f n_{cell}^{-1}})^{-1} \tag{11}$$

where n_{cell} is the total number of the cells in S layer. Since J_f is greater than or equal to zero (as equation 7 is a sum of absolute value), the sigmoid membrane potential $LGMD_f$ varies from 0.5 to 1. The collision alarm is decided by the spiking of cell LGMD. If the membrane potential $LGMD_f$ exceeds the threshold Ts, a spike is produced. A certain number of successive spikes, which is denoted by S_{LGMD}, will trigger the collision alarm in the LGMD cell. Of course, in the modified model, collision alarm is only triggered under the condition that $\tilde{D} = 1$ where the moving object is approaching. The spikes may be suppressed by the FFI cell when whole field movement occurs [18].

3.1.7 FFI cell

If it is not suppressed during turning, the network may produce spikes and even false collision alerts due to sudden changes in the visual scene. The feed forward inhibition and lateral inhibition work together to cope with such whole field movement [18]. The FFI excitation at the current frame is gathered from the photoreceptor cells with one frame delay,

$$F_f = \sum_{j}^{n_a} \alpha_{f-j}^{F} F_{f-j} + \sum_{x=1}^{n_r} \sum_{y=1}^{n_c} abs(P_{f-1}(x, y)) n_{cell}^{-1} \tag{12}$$

where α_{f-j}^{F} is the persistence coefficient for FFI and $\alpha_{f-j}^{F} \in (0, 1)$, n_a defines how many time steps the persistence can last.

Once F_f exceeds its threshold T_{FFI}, spikes in the LGMD are inhibited immediately. The threshold T_{FFI} is also adaptable,

$$T_{FFI} = T_{FO} + \alpha_{ffi} T_{FFI_{f-1}} \tag{13}$$

where T_{FO} is the initial value of the T_{FFI}, the adaptable threshold is decided by the previous T_{FFI} and α_{ffi} is a coefficient. It should be mentioned here that the parameters here such as T_{FO}, α_{ffi} are set are set truly based on the situation of the real world applications. It is strongly depends on the type or style of the camera's movement. It is also affected by the size of the image frame. In the case when the camera is nearly stable, FFI cell is normally ignored as it is nearly kept same.

As described in this section, the modified neural network model for LGMD only involves low level image processing, such as excitation transfer and neighborhood operations; computationally expensive methods, such as object recognition or scene analysis, are not used. Consequently, the proposed neural network model is able to work in real time and is independent of object classification.

3.2 Simulation results on the proposed model

Two different data sets were used to test the efficiency and stability of the proposed neural network model for LGMD. The first experiment is on a simulated data set that demonstrates approaching and receding movements. The second data sets are two recorded video clips. The parameters such as thresholds and inhibition weights were kept the same in all experiments. The simulation was performed using the MATLAB environment.

3.2.1 Results on simulated data set

We create a sequence that contain 125 images with the approaching and receding movement of a square object. Some image frames are shown in figure 2 with image size 150×100. The square object with an initial size of 3×3 starts to approach from frame 5 to frame 41 and then recedes from frame 41 to frame 79. The square object increase or decrease its border by 2 pixels (1 pixel on each side) per frame. From frame 79 to frame 84, the square object is kept at same size of 3×3. Then the object approaches from frame 84 to frame 101 and then recedes from frame 101 to frame 120. This time, the square object increases or decreases its border by 4 pixels (2 pixel on each side) per frame. The square object is kept at same size, 3×3, from frame 120 to frame 125.

Figure 3 shows the output of the modified LGMD neural network model on the simulated sequence shown in figure 2. The vertical axis is the normalized membrane potentials of the LGMD cell. It is identical to the previous LGMD based neural network model. The other output of the proposed neural network is the direction of the depth movement, represented by the markers on the normalized membrane potentials of the LGMD cell; '△' indicates an

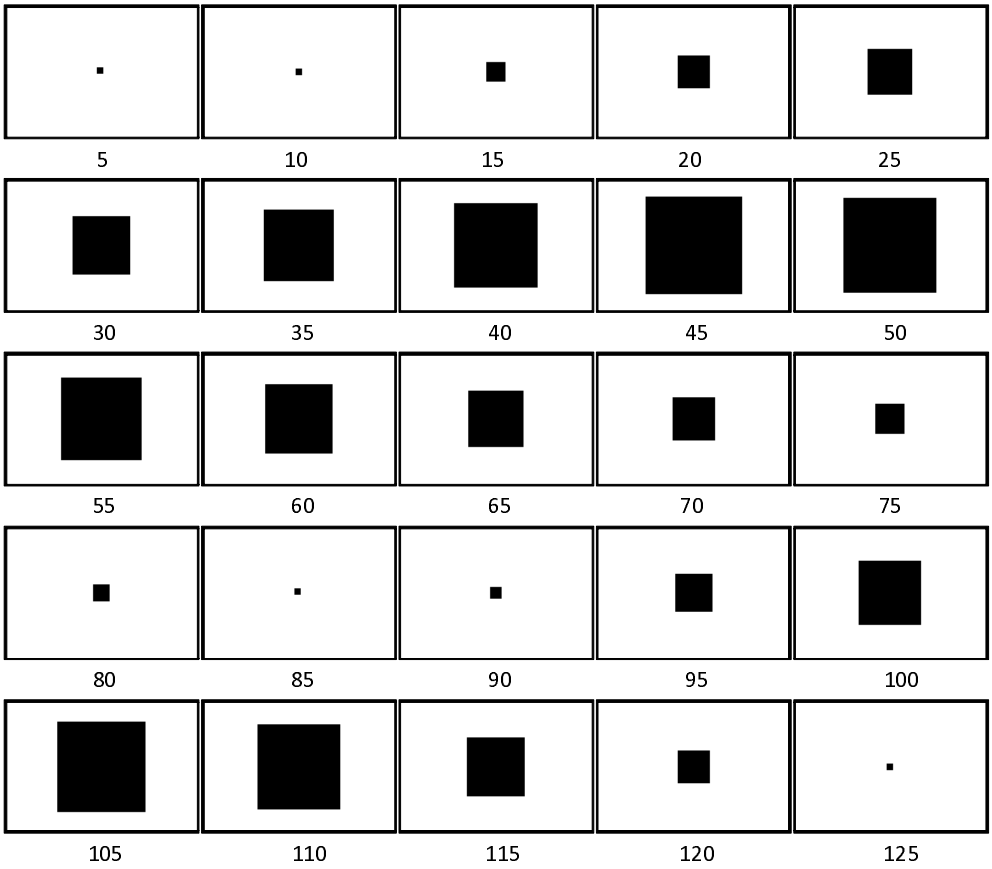

Fig. 2. The simulated sequence generated in the experiment. In the first part the square object first grows in size, then shrinks; this process is repeated in the second part at higher speed.

approaching object, '▽' a receding object and '◯' no significant movement. From figure 3, we can clear see that the output of the proposed LGMD neural network model works very well on the simulated data set.

3.2.2 Results on real recorded data

We recorded two short video clips (shown in figures 4 and 6 respectively) for the second experiment, using 320×240 gray scale images. In these two recorded videos (4), a ball is shown, mainly receding to the chair and then bouncing back to approach the camera. There are 18 and 21 frames in the first and second sequences respectively. The first recording has a bigger, fast-moving ball while the second has a smaller, slower-moving ball.

Figure 5 and 7 show the output of the modified modified LGMD based neural network model on the recorded sequences shown in figure 4 and 6 respectively. The vertical axis gives the normalized membrane potentials of the LGMD cell. It is identical to the previous LGMD based neural network model. The other output of the proposed neural network is the direction of the depth movement,

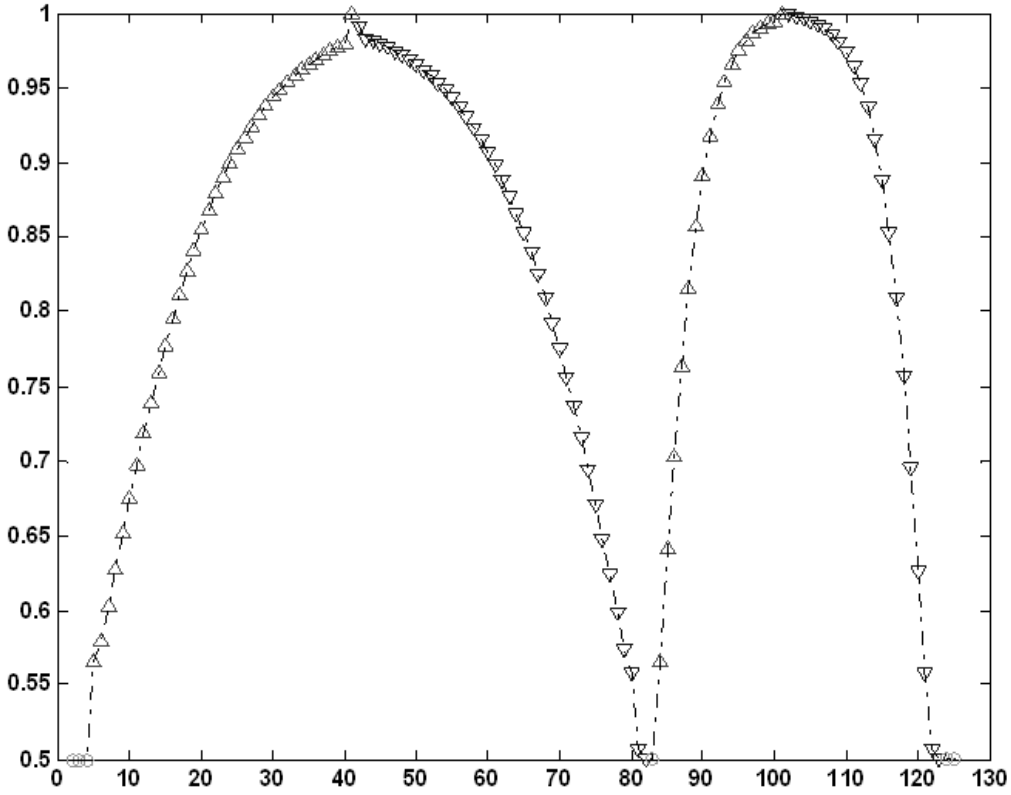

Fig. 3. The output of the modified LGMD based neural network model on the simulated sequence shown in figure 2. The vertical axis shows the normalized membrane potentials of the LGMD cell; the markers denote the depth movement direction of the object. '△' denotes an approaching; '▽' a receding object and '◯' no significant movement.

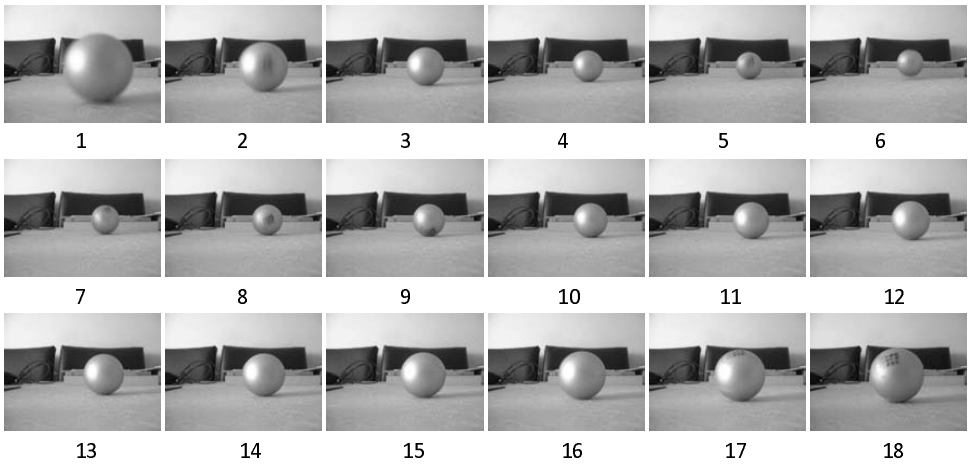

Fig. 4. The first recorded sequence used in the experiment. There are 18 frames featuring a ball receding from the camera and then bouncing back to the camera after it hits a chair.

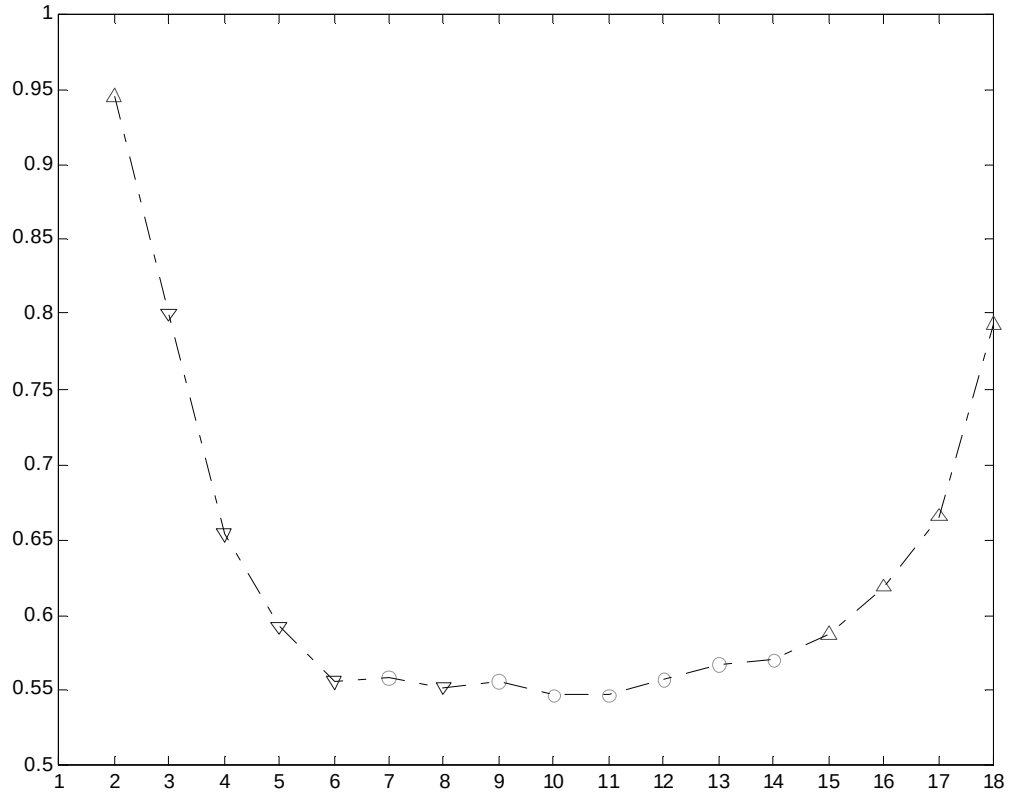

Fig. 5. The output of the modified LGMD based neural network model on the first recorded sequence shown in figure 4. The vertical axis is the normalized membrane potentials of the LGMD cell. The markers denote the depth movement direction; '△' denote approaching objects; '▽' receding objects and '◯' no significant movement.

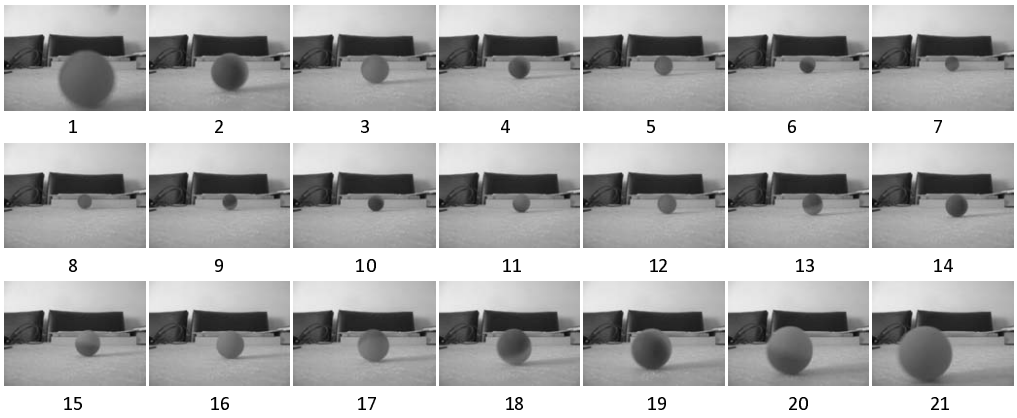

Fig. 6. The second recorded sequence used in the experiment. There are 21 frames, featuring a ball receding from the camera and then bouncing back towards the camera after it hits the chair.

represented by the markers on the normalized membrane potentials of the LGMD cell; '△' denotes an approaching object; '▽' a receding object and '◯' no significant movement. From figure 5 and 7, we can clear see that the proposed LGMD neural network model works very well on both the two

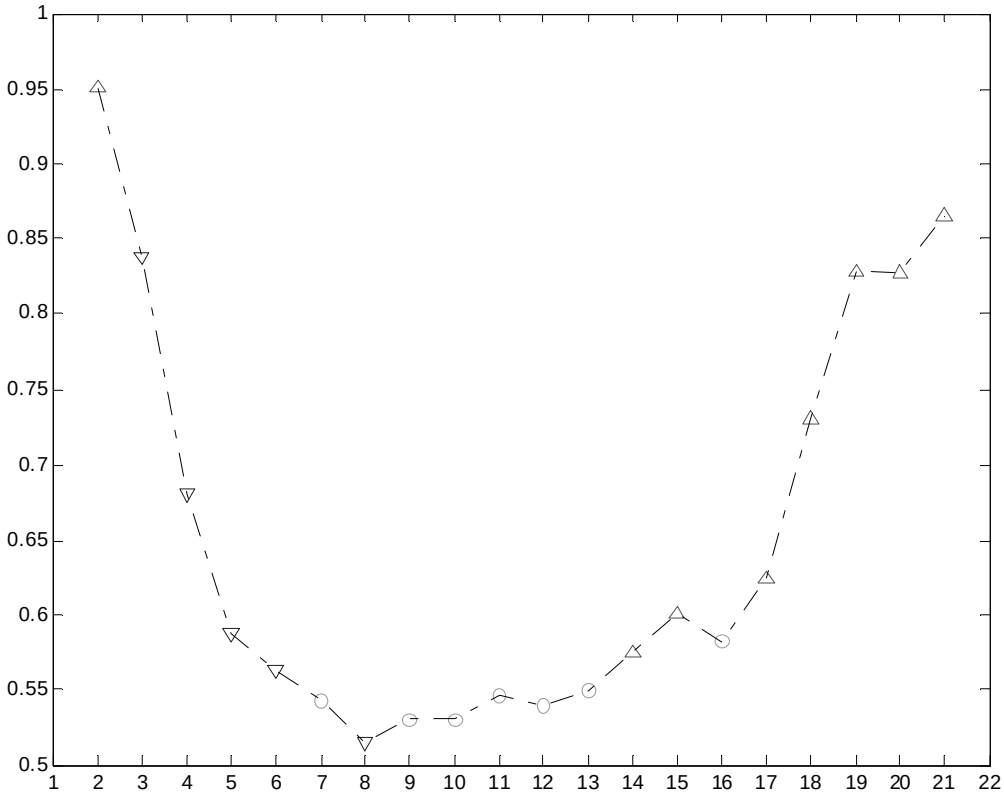

Fig. 7. The output of the modified LGMD based neural network model on the second recorded sequence shown in figure 6. The vertical axis is the normalized membrane potentials of the LGMD cell. The markers denote the depth movement direction; '△' denote approaching objects; '▽' receding objects and '◯' no significant movement.

recorded data sets, although the speed of the movements are different in these two recordings.

4 Hardware design and implementation

The entire collision detection algorithm, based on the modified LGMD as presented in section 3 has been implemented on a Field Programmable Gate Array (FPGA). Rather than a mixed digital/analogue implementation of the LGMD[8,9], an all digital implementation of a modified version is presented.

4.1 Overall architecture and platform

The high-level block diagram of the overall architecture of the system has been shown on figure 8. The real-time video stream is inputed from a digital camera into the FPGA chip. It is displayed on an monitor and its frames are

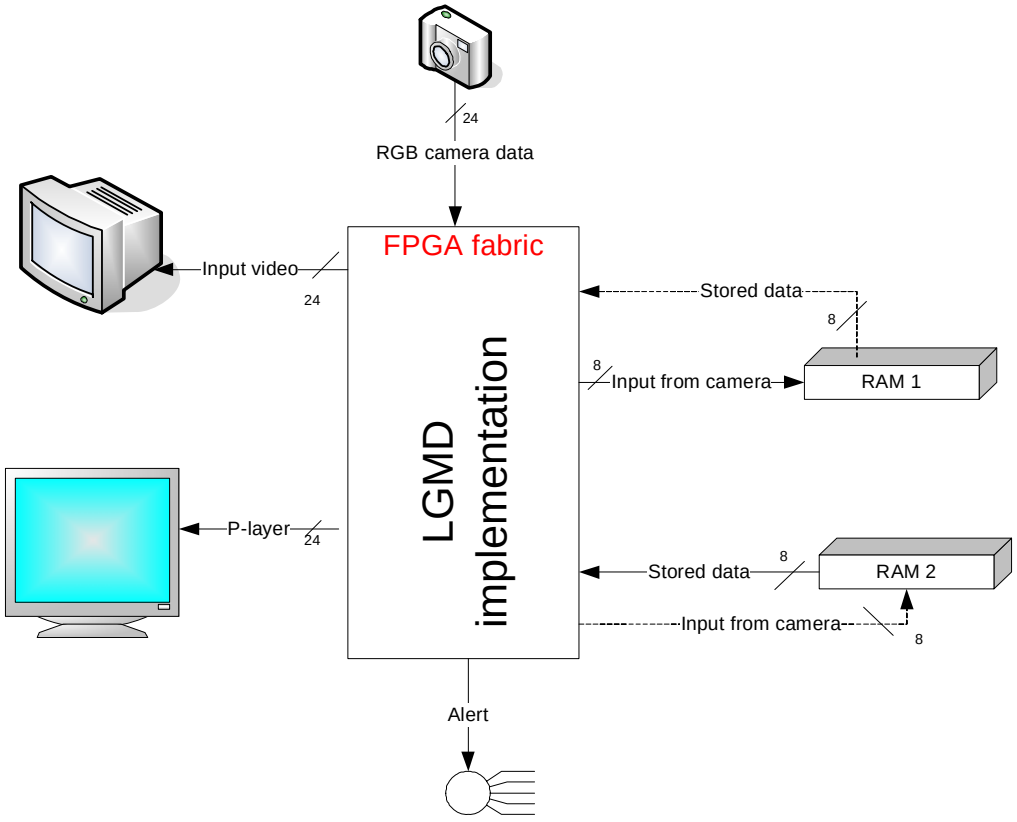

Fig. 8. A high-level block diagram of the FPGA implementation of the modified LGMD model.

transfered to gray scale images that are stored in two external RAMs. The neural computing is carried out on the FPGA chip and the excitation S-layer is displayed on another monitor and an alert is also given out.

Figure 9 shows the system setup that runs the modified LGMD model in real-time situation. It includes a Celoxica RC340 board, a digital camera and two monitors. The modified LGMD model lights up the LEDs (flash lights) on the FPGA board based on the values of both LGMD cell and D cell that are also shown on the LCD of the FPGA board.

The overall architecture has fully been accomplished on a Celoxica RC340 prototyping board shown on figure 9; packaged with Xilinx Virtex-4 XC4VLX160, embedded Block RAM totaling 5,184 Kbits and four banks of ZBT RAM totaling 32MB, LCD, LEDs and multiple video input and output ports.

4.2 FPGA design

The whole circuitry on the FPGA design as shown in figure 10 has five blocks; the input, P-layer, S-layer, J cell and the D cell. The input and P-layer blocks

Fig. 9. The system setup includes a Celoxica RC340 board, a digital camera and two monitors. The modified LGMD model lights up the LEDs (flash lights) on the FPGA board based on the values of both LGMD and D cells. These values are also shown on the LCD of the FPGA board.

runs in parallel whiles the S-layer gets triggered when the entire frame has been processed.

The input block reads real-time camera data in 24 bit RGB format and converts it into 8 bit Grayscale intensity. The 8 bit intensity value is written into one of the available RAM blocks whiles the corresponding stored data is read from the other RAM block, serving as the previous pixel value. The 10 bit x-location and y-location address is also use to address the store data in RAM. The two block of RAM are used to buffer input data from the camera.

The current pixel value (from the camera) and the previous pixel value (from RAM) are used to estimate the luminance P-layer value for the corresponding pixel. This three stage pipeline is completed when an entire frame is captured. The excitatory S-layer is then triggered. This layer uses all 8 neighboring pixels in the P-layer. The architecture implemented here is as shown in figure 11. Pixel data from the three rows involved in the computation are copied into a buffer one after the other. The S-layer for each pixel takes exactly 3 clock cycles, the same number of cycles required to fill the three buffers.

The processing requires a maximum of seven comparators arranged in a chain as shown in figure 11 and begins execution as soon as the buffer is full. From

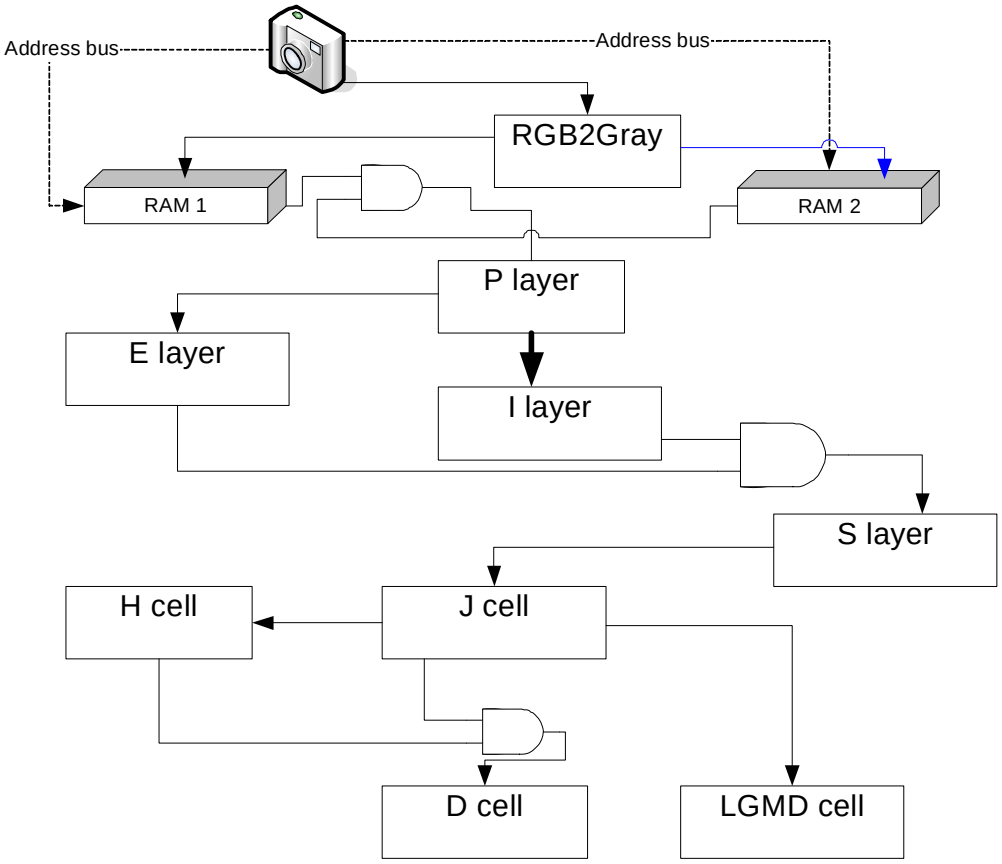

Fig. 10. A high-level circuitry diagram of the various blocks on FPGA

figure 11, the shaded pixels in the second row are the pixel whose corresponding S-layer value will be generated after three clock cycles.

The S-layer data is passed over to the most iterative block; the J cell, which sums all the pixels values from the S-layer. This block runs in parallel with the S-layer and uses a single accumulator. The J cell in conjunction with the H cell is used to generate the value for the D cell. The D cell uses the H cell, which is the delayed J cell values as shown in figure 10.

In addition, a Lookup Table (LUT) is used to estimate the intensity of the LGMD cell, which triggers an alarm should the value exceeds a threshold. The reason is that the equation 11 is very difficult to to be implemented on FPGA directly as there are both exponential and division functions in it. In order to get an efficient LUT, equation 11 was rewritten to equation 14. The expected values of the $LGMD$ cell are chosen as $\{0.50, 0.51, 0.52, \cdots, 0.99, 1.00\}$. So a LUT with 51 outputs that is related to the 51 values of $LGMD$ is built. The associated values of J are calculated and stored into the LUT. During the implementation, the obtained value of the J cell is compared with the values in the LUT and the closest value will be found and its associated value in

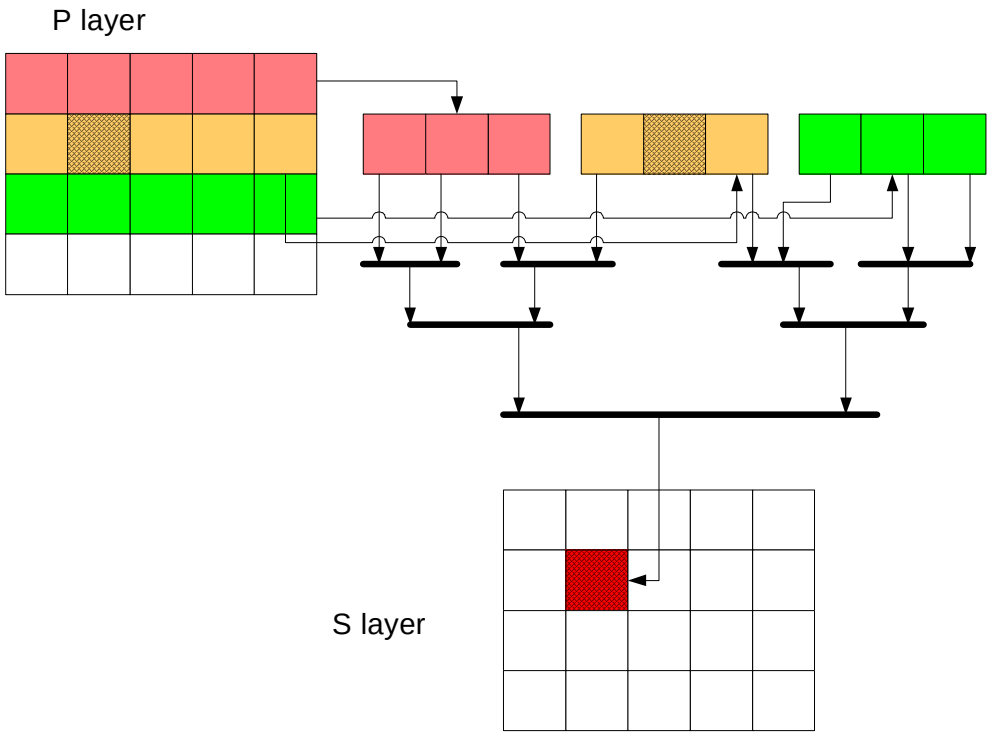

Fig. 11. A detailed translation of the p-layer into s-layer

LUT for $LGMD$ will be taken.

$$J_f = -\ln(LGMD_f^{-1} - 1) \times n_{cell} \tag{14}$$

All the layers in the modified LGMD have been implemented on the FPGA fabric with the use of the Block RAM, making it possible to address each layer like a dual-port memory block. The implementation in hardware excludes the FFI cell as shown in figure 1. The reason is that the FFI cell is only useful when the camera is moving. In current implementation, it was ignored. However, it can be easily added into the system without any difficulty as there is not any complex operations in its computing. The hardware implementation rather makes use of a predefined threshold to estimate the excitation. Again, the excitation of the LGMD cell in figure 11 is very dependent on the D cell. If the value of the D cell is other than 1 (approaching); thus if the object is stationary or receding, there is no alert generated at the LGMD cell.

The resources used by the FPGA implementation of the proposed model for the LGMD neuron is listed in the table 1. It was implemented on a Xilinx Virtex-4 *XC4VLX160* chip, package *FF1148* and speed grade *-10*.

Table 1
Implementation results for the modified LGMD, using Virtex-4 *XC4VLX160*, package *FF1148* and speed grade *-10*.

Resource		**Total Used**	
Name	**Total**	**Used**	**Per.(%)**
Flip Flops	135,168	2,325	1
4 input LUTs	135,168	3,001	2
bonded IOBs	768	355	46
Occupied Slices	67,584	3,206	4
RAM16s	288	285	98

4.3 Hardware testing results

The implementation has been tested with two frame sizes, 300×200 and 600×400. The maximum attainable clock frequency is 50MHz, with 40MHz being the highest stable frequency. The design takes a total of $3N+7$ cycles to completely generate an LGMD output, where N is the number of pixels in the entire frame. For frame size 300×200 running at 40MHz, the system processes approximately 222 frames per second; for frame size 600×400 the value reduces to 55 frames per second. The low resource utilization of the implementation makes it possible to run multiple LGMD at the same frequency.

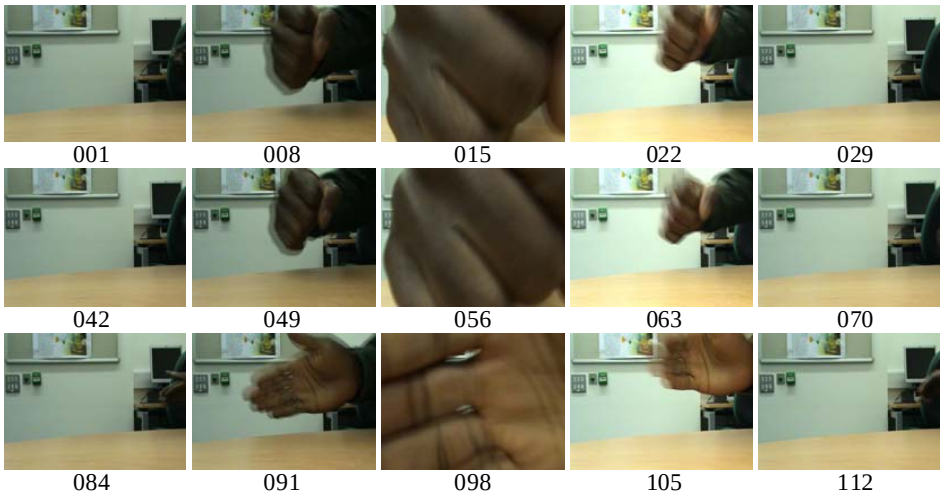

Fig. 12. Some frame samples from a video clips that recorded a hand movement in front of the digital camera. The frame numbers are shown under each frame. It was input into the FPGA board while the FPGA implementation of the modified LGMD model running. The total number of frames of this example are 115. The frame size is 600×400 and frame rate is 25.

The high computational efficiency makes it possible for the modified LGMD to be used in visual sensor systems with very high frame rate and/or high

image resolution. On a commercial FPGA board with visual input/output, it works very well as a fast motion detector.

The reported clock frequency of 40MHz to 50MHz also includes the design for controlling the external logic for the 2 VGAs, the camera input and the LEDs for alerts. The design and verification was accomplished using Handel-C high level descriptive language. Compilation and simulation were achieved using the Agility DK design suite. Synthesis, the translation of abstract high-level code into a gate-level netlist was accomplished using Xilinx ISE tools. The table 1 gives the details of the resource utilization of the FPGA implementation.

Figure 12 show some video frame that we test the hardware implementation. The object (hand) moves in front of the camera and there are three times approaching and receding respectively. The video are recorded into the digital camera and the outputs of the LGMD and D cells were written into the external memory. Figure 12 show some frames from the selected 115 frames in the recored video clip.

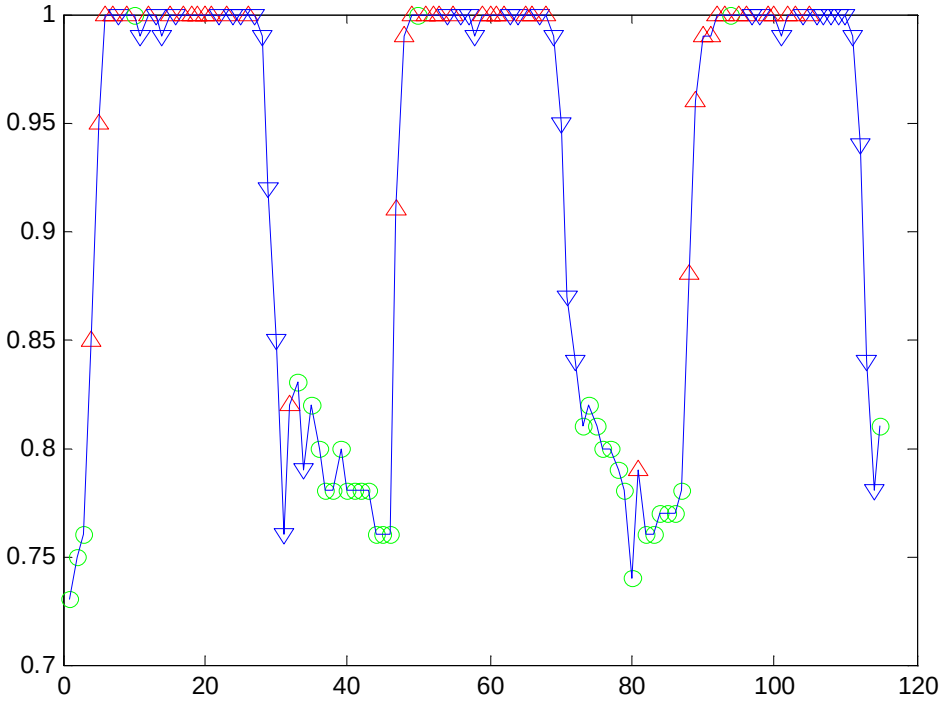

Fig. 13. Experimental results read from external memory of the FPGA board. The video frames were showed in figure 12. In this example, hand movement in front of the camera is connected to the FPGA board. The vertical axis is the normalized membrane potentials of the LGMD cell. The markers denote the depth movement direction; '△' denote approaching objects; '▽' receding objects and '◯' no significant movement.

The outputs of the LGMD cell and D cell were read out from the external memory on the prototyping board. The results were drawn in figure 13. The vertical axis is the normalized membrane potentials of the LGMD cell. The

markers denote the depth movement direction; '△' denote approaching objects; '▽' receding objects and '◯' no significant movement. From this figure, we can see clearly that the FPGA implementation of the system worked very well in response to this object movement. In comparison with the software simulation results in previous section such as figure 5, the curve is not as smooth as the one in figure 5. the reason is that we used a very small LUT during the computing of LGMD values. Nevertheless, this implementation can definitely fulfill the task of giving correct alarms.

5 Conclusion

In this paper, we proposed a modified neural network model for LGMD that provides additional information on the depth direction of the movement. The modified model is created and designed based on the previous LGMD models and just adds very little extra computational cost. It has some layers in common with the previous LGMD model, allowing efficient neural computation. The proposed LGMD model can recognize whether the object is approaching or receding very quickly.

The proposed modified LGMD model has been designed on the Xilinx FPGA chip. The architecture is designed for the general purposes that can be transfered to any other FPGA device. The whole design is compact and only occupy very limited hardware resources. It has been tested based on real-time video stream and worked very well. Experimental results showed it was very coherent with the software simulation results.

The high computational efficiency makes it possible for the modified LGMD to be used in visual sensor systems with very high frame rate and/or high image resolution. The whole system worked as a fast motion detector with quick response from the movement in front of the camera. The FPGA implementation on a general purpose hardware platform makes it suitable for application in various situations.

The future research will be a complete LGMD chip combining the proposed LGMD model here with the specialized translation-sensitive neural network (TSNN) model. It will provide both translation and depth movement information for LGMD and will work as a truly motion sensor.

6 Acknowledgments

The authors would like to thank the UK Trade and Strategy Board for supporting the project under the program grant TP/2/SC/6/I/10444.

References

[1] Sergi Bermudez i Badia, Pawel Pyk, and Paul F.M.J. Verschure. A fly-locust based neuronal control system applied to an unmanned aerial vehicle: the invertebrate neuronal principles for course stabilization, altitude control and collision avoidance. *The International Journal of Robotics Research*, 26(7):759–772, 2007.

[2] M. Blanchard, F.C. Rind, and P.F.M.J. Verschure. Collision avoidance using a model of the locust lgmd neuron. *Robotics and Automonous Systems*, 30:17–38, 2000.

[3] M. J. Blanchard, F. C. Rind, and P. F. M. J. Verschure. Using a mobile robot to study locust collision avoidance responses. *International journal of neural systems*, 9:405 – 410, 1999 1999. ID: 53; ID: 601.

[4] Mark Blanchard, Paul F. M. J. Verschure, and F. Claire Rind. Using a mobile robot to study locust collision avoidance responses. *Int. J. Neural Syst.*, 9(5):405–410, 1999.

[5] J. Cuadri, G. Linan, R. Stafford, M. S. Keil, and E. Roca. A bioinspired collision detection algorithm for vlsi implementation. volume 5839, pages 238–248. SPIE, 2005.

[6] Sergi Bermudez i Badia and Paul F.M.J. Verschure. A collision avoidance model based on the lobula giant movement detector neuron of the locust. In *proceedings of IJCNN*, pages 1757–1761, 2004.

[7] S Judge and F Rind. The locust DCMD, a movement-detecting neurone tightly tuned to collision trajectories. *Journal of Experimental Biology*, 200(16):2209–2216, 1997.

[8] R. Laviana, L. Carranza, S. Vargas, G. Linan, and E. Roca. A bioinspired vision chip architecture for collision detection in automotive applications. In R. A. Carmona and G. Linan-Cembrano, editors, *Society of Photo-Optical Instrumentation Engineers (SPIE) Conference Series*, volume 5839 of *Society of Photo-Optical Instrumentation Engineers (SPIE) Conference Series*, pages 13–24, June 2005.

[9] Hirotsugu Okuno and Tetsuya Yagi. Real-time robot vision for collision avoidance inspired by neuronal circuits of insects. In *IROS*, pages 1302–1307, 2007.

[10] Hirotsugu Okuno and Tetsuya Yagi. A visually guided collision warning system with a neuromorphic architecture. *Neural Networks*, 21(10):1431–1438, 2008.

[11] F. C. Rind, R. D. Santer, M. J. Blanchard, and P. F. M. J. Verschure. *Locust looming detectors for robot sensors*. Springer, Berlin, 2003 2003. ID: 75; ID: 2921.

[12] F. C. Rind and P. J. Simmons. Orthopteran dcmd neuron: a reevaluation of responses to moving objects. i. selective responses to approaching objects. *J Neurophysiol*, 68(5):1654–1666, 1992.

[13] F. Claire Rind. A directionally selective motion-detecting neurone in the brain of the locust: physiological and morphological characterization. *Journal of Experimental Biology*, 149:1–19, 1990.

[14] F. Claire Rind. Identification of directionally selective motion-detecting neurones in the locust lobula and their synaptic connections with an identified descending neurone. *Journal of Experimental Biology*, 149:21–43, 1990.

[15] F. Claire Rind and Peter J. Simmons. Seeing what is coming: building collision-sensitive neurones. *Trends in Neurosciences*, 22:215–220, 1999.

[16] F.C. Rind and D.I. Bramwell. Neural network based on the input organization of an identified neuron signaling impending collision. *Journal of Neurophysiology*, 75:967–985, 1996.

[17] R. D. Santer, P. J. Simmons, and F. C. Rind. Gliding behaviour elicited by lateral looming stimuli in flying locusts. *Journal of comparative physiology. A, Neuroethology, sensory, neural, and behavioral physiology*, 191(1):61–73, January 2005.

[18] R. D. Santer, R. Stafford, and F. C. Rind. Retinally-generated saccadic suppression of a locust looming detector neuron: Investigations using a robot locust. *Journal of the Royal Society: Interface*, 1:61–77, 2004.

[19] Shigang Yue and F. Claire Rind. A collision detection system for a mobile robot inspired by the locust visual system. In *ICRA*, pages 3832–3837, 2005.

[20] Shigang Yue and F. Claire Rind. Collision detection in complex dynamic scenes using an lgmd-based visual neural network with feature enhancement. *IEEE Transactions on Neural Networks*, 17(3):705–716, 2006.

[21] Shigang Yue and F. Claire Rind. Visual motion pattern extraction and fusion for collision detection in complex dynamic scenes. *Computer Vision and Image Understanding*, 104(1):48 – 60, 2006.

[22] Shigang Yue and F. Claire Rind. A synthetic vision system using directionally selective motion detectors to recognize collision. *Artificial Life*, 13(2):93–122, 2007.

[23] Shigang Yue, F. Claire Rind, Matthias S. Keil, Jorge Cuadri, and Richard Stafford. A bio-inspired visual collision detection mechanism for cars: Optimisation of a model of a locust neuron to a novel environment. *Neurocomputing*, 69(13-15):1591–1598, 2006.